ACS chemical biology

Letters

pubs.acs.org/acschemicalbiology

Identification of Small-Molecule Antagonists of the *Pseudomonas aeruginosa* Transcriptional Regulator PqsR: Biophysically Guided Hit Discovery and Optimization

Tobias Klein,[†,#] Claudia Henn,[†,#] Johannes C. de Jong,[†] Christina Zimmer,[†] Benjamin Kirsch,[†] Christine K. Maurer,[†] Dominik Pistorius,[†] Rolf Müller,[†,§] Anke Steinbach,[†] and Rolf W. Hartmann*[,†,‡]

[†]Helmholtz-Institute for Pharmaceutical Research Saarland (HIPS), Campus C2.3, 66123 Saarbrücken, Germany

Departments of [‡]Pharmaceutical and Medicinal Chemistry and [§]Pharmaceutical Biotechnology, Saarland University, Campus C2.3, 66123 Saarbrücken, Germany

Supporting Information

ABSTRACT: The Gram-negative pathogen *Pseudomonas aeruginosa* produces an intercellular alkyl quinolone signaling molecule, the *Pseudomonas* quinolone signal. The *pqs quorum sensing* communication system that is characteristic for *P. aeruginosa* regulates the production of virulence factors. Therefore, we consider the *pqs* system a novel target to limit *P. aeruginosa* pathogenicity. Here, we present small molecules targeting a key player of the *pqs* system, PqsR. A rational design strategy in combination with surface plasmon resonance biosensor analysis led to the identification of PqsR binders. Determination of thermodynamic binding signatures and functional characterization in *E. coli* guided the hit optimization, resulting in the potent hydroxamic acid derived PqsR antagonist **11** (IC_{50} = 12.5 μM). Remarkably it displayed a comparable potency in *P. aeruginosa* (IC_{50} = 23.6 μM) and reduced the production of the virulence factor pyocyanin. Beyond this, site-directed mutagenesis together with thermodynamic analysis provided insights into the energetic characteristics of protein−ligand interactions. Thus the identified PqsR antagonists are promising scaffolds for further drug design efforts against this important pathogen.

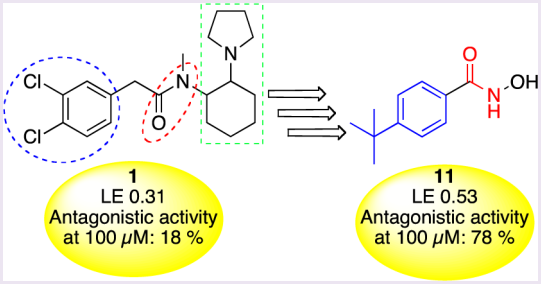

Pseudomonas aeruginosa is an environmental highly adaptable opportunistic pathogen that is one of the leading causes for nosocomial infections[1] and is responsible for chronic lung infections in the majority of cystic fibrosis patients.[2] It coordinates group behaviors *via* a cell-density-dependent cell-to-cell communication system known as *quorum sensing* (QS).[3] Beside the *las*[4,5] and the *rhl*[6,7] communication systems, which use *N*-acyl homoserine lactones as autoinducers, *P. aeruginosa* employs a characteristic *pqs* QS system.[8] It functions *via* the signal molecules PQS (2-heptyl-3-hydroxy-4-quinolone) and its precursor HHQ (2-heptyl-4-quinolone) that interact with their receptor PqsR to control the production of a number of virulence factors such as pyocyanin and biofilm formation.[9−11] Due to growing antibiotic resistance there is an urgent need for therapeutics with novel modes of action. Targeting bacterial virulence or disrupting the interaction between the host and the pathogen are attractive options that are increasingly being explored.[12] Therefore we consider PqsR a novel, promising target to disrupt PqsR-dependent gene expression, thereby limiting *P. aeruginosa* pathogenicity without affecting bacterial viability.[13] Recently, we reported on the discovery of the first PqsR antagonists.[14] However, as their structures are derived from the natural effector HHQ, they have insufficient physicochemical properties to be used as a drug. Here, we describe the discovery and optimization of small molecules targeting the transcriptional regulator PqsR using a rational design strategy guided by biophysical methods. Combination of site-directed mutagenesis and thermodynamic analysis enabled us to study protein−ligand interactions in detail.

The κ-opioid receptor agonist (±)-*trans*-U50488 (**1**) was recently found to stimulate the transcription of *pqsABCDE* in *P. aeruginosa* PAO1, indicating that it could act *via* PqsR.[15] Employing surface plasmon resonance (SPR) biosensor analysis and isothermal titration calorimetry (ITC), we confirmed that **1** binds to PqsR (Figure 1; Supplementary Figures S1 and S2) thereby providing a promising starting point for the identification of small-molecule PqsR ligands.

We applied a rational design strategy that involves the simplification of **1** into smaller fragments and analogues. In the context of antibacterial drug discovery, fragment-based design is a promising strategy since it makes it possible to address the key issues, namely, insufficient physicochemical properties and lack of chemical diversity.[16,17] The derived in-house library included (**i**) *N*-heteroaromatic substituted benzamides, (**ii**) substituted benzyl- and benzamides, and (**iii**) *N*-phenyl substituted isonicotin- and nicotinamides (Figure 1). Screening

Received: February 15, 2012
Accepted: June 20, 2012
Published: July 5, 2012

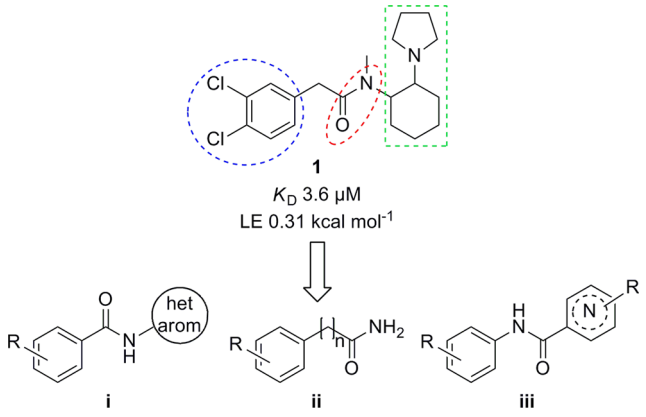

Figure 1. Ligand-based design strategy. Structure of the PqsR ligand (±)-*trans*-U50488 **1** (top) and general structures **i**–**iii** of the derived focused library (below). K_D value and ligand efficiency (LE) were determined using ITC.

of the focused library (106 compounds) in a SPR biosensor assay monitoring the affinity toward PqsR revealed binders including four top candidates with outstanding ligand efficiencies (LE, Figure 2).

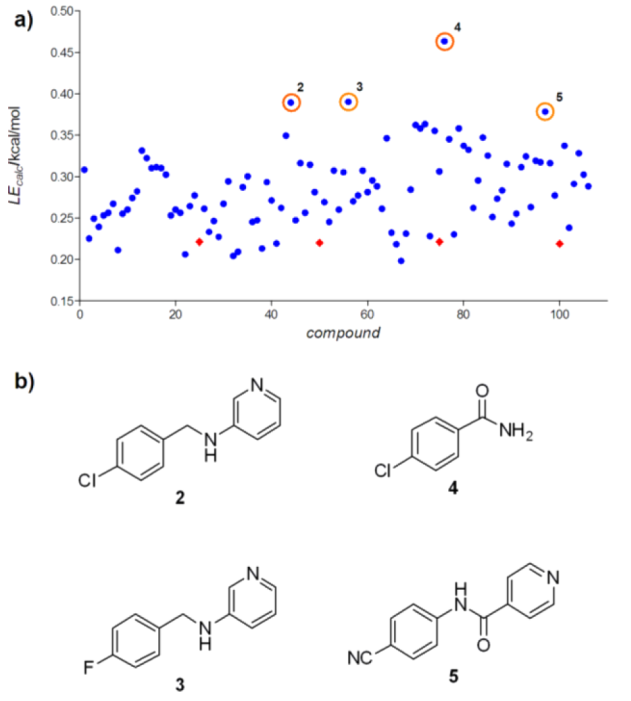

Figure 2. SPR screening data analysis. (a) Processed single point binding data for compounds, referenced for blanks, DMSO calibration, and streptavidin reference flow cell; blue dots represent calculated LE for compounds; red squares represent calculated LE for positive control **1** (referring surface stability); orange circles represent screening hits. Compounds were injected at 100 μM. (b) Chemical structures of the top four hits.

The major drawback of screening small simple molecules is that the binding affinity is usually low.[17] Therefore, LE, which is calculated as the binding energy of the ligand per heavy atom thereby normalizing the affinity and molecular size of a compound, was used for effective hit selection.[18] To account for heteroatoms the binding efficiency index (BEI), that engages the total molecular weight instead of the number of non-hydrogen atoms[19] is superior but here the ranking did not change. To verify and further characterize the best hit **4**, we carried out a thermodynamic analysis and evaluated its agonistic and antagonistic activity (Table 1). Using ITC a dissociation constant (K_D) of 25.5 μM was determined for **4** binding to PqsR and the LE of 0.63 kcal mol^{-1} confirmed the high potential of **4** as starting point for optimization. Further, we examined the PqsR-mediated transcriptional effect in a heterologous reporter gene assay in *E. coli*.[20] The latter was used as it provides a system to characterize the functionality of PqsR ligands independent of the entire *pqs* system present in *P. aeruginosa*.[21] Remarkably, in the *E. coli* assay **1** did not stimulate the transcription of *pqsABCDE* as described,[15] rather it acts as a weak PqsR antagonist. More importantly, for ligand **4** a significant reduction of the PqsR stimulation was observed. Considering the promising LE and the antagonistic activity compound **4** was chosen as starting point for structural modifications.

Variation of the length of the alkyl chain in PQS[21,22] as well as in HHQ and its derivatives[14] demonstrated a chain length dependency of agonistic and antagonistic activities revealing the alkyl chain as a key feature. Therefore, alkyl chains varying from C1 to C4 were introduced in the *para*-position of the benzamide core that led to compounds **6**–**10** (Table 1; Supplementary Figure S3). Compared to **4** (K_D = 25.5 μM) the *tert*-butyl substituted benzamide (**9**, K_D = 0.9 μM) showed a 29-fold increase in binding affinity, and the LE remained constant at a value of 0.63 kcal mol^{-1}. However, changing the constitution from *tert*- to isobutyl (compound **10**, K_D = 5.7 μM) reduced the affinity again. Analysis of the thermodynamic signatures revealed that ligands **7**–**10** are enthalpy driven binders indicating a good noncovalent bond complementary between the protein and the compounds.[23] However, with increasing enthalpic contribution in this series the entropic terms became more unfavorable, thereby partially compensating the enthalpic gain (Supplementary Figure S4).

The replacement of the Cl-substituent in *para*-position of **4** by alkyl residues (compounds **6**–**10**) inverted the functional properties from antagonistic (**4**) to agonistic activity (**6**–**10**). Interestingly, the ligands with the bulkiest substituents **9** and **10** showed in addition to their moderate agonistic activity a significant reduction of the PqsR stimulation. These findings demonstrate the impact of the alkyl moiety on binding affinity as well as on functional properties.

In order to elucidate the role of the amide function, we exchanged it by a hydroxamic acid in the ligand with the highest affinity and the most favorable enthalpic contribution (compound **9**). The resulting compound **11** (K_D = 4.1 μM) displayed a 4.6-fold reduced affinity compared to that of **9** that is due to a decrease in ΔH. Interestingly, the antagonistic potency was improved, and the agonistic activity was completely lost. To investigate whether in the alkyl-substituted series the replacement of the amide by a hydroxamic acid in general can turn agonists into antagonists, the corresponding derivative of **7** (compound **12**) was synthesized. Indeed, **12** (K_D = 19.7 μM) is also a pure PqsR antagonist.

Combining ITC with site-directed mutagenesis provides a valuable thermodynamic tool to identify the effects of specific residues in interaction with ligands.[24] Gln194, the only polar residue in the PQS-binding pocket (Williams, P. University of Notthingham, Nottingham, U.K. Personal communication, 2011), was mutated, and the binding of **1**, **8**, **9**, and **11** to

dx.doi.org/10.1021/cb300208g | *ACS Chem. Biol.* 2012, 7, 1496–1501

Table 1. Thermodynamic Parameters of Ligands 1, 4, and 6−12 Binding to PqsR and Their Agonistic and Antagonistic Activities[a]

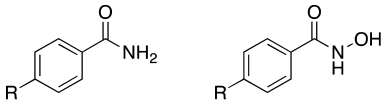

4, 6-10 11, 12

ligand	R	K_D [μM]	ΔG [kcal mol^{-1}]	ΔH [kcal mol^{-1}]	$-T\Delta S$ [kcal mol^{-1}]	LE [kcal mol^{-1}]	agonistic activity [%]	antagonistic activity [%]
1		3.6 ± 0.4	−7.4 ± 0.1	−4.7 ± 0.1	−2.7 ± 0.1	0.31	n.a.	18 ± 3[c]
4	Cl	25.5 ± 2.5	−6.3 ± 0.1	−4.1 ± 0.2	−2.1 ± 0.2	0.63	n.a.	53 ± 7[c]
6	Me	31.2 ± 3.4	−6.1 ± 0.1	−2.2 ± 0.1	−3.9 ± 0.1	0.62	33 ± 2[b]	n.i.
7	Et	7.3 ± 0.6	−7.0 ± 0.1	−4.6 ± 0.3	−2.4 ± 0.3	0.64	122 ± 13[b]	n.i.
8	*i*Pr	3.0 ± 0.4	−7.5 ± 0.1	−6.3 ± 0.3	−1.3 ± 0.4	0.63	111 ± 10[b]	n.i.
9	*t*Bu	0.9 ± 0	−8.3 ± 0	−9.7 ± 0.3	1.5 ± 0.3	0.63	43 ± 3[b]	48 ± 1[b]
10	*i*Bu	5.7 ± 0.9	−7.2 ± 0.2	−7.9 ± 0.4	0.7 ± 0.1	0.55	32 ± 3[c]	45 ± 8[c]
11	*t*Bu	4.1 ± 0.6	−7.4 ± 0.1	−8.9 ± 0.2	1.5 ± 0.3	0.53	n.a.	78 ± 12[c]
12	Et	19.7 ± 1.2	−6.4 ± 0	−4.8 ± 0.2	−1.6 ± 0.2	0.54	n.a.	50 ± 9[b]

[a]ITC titrations were performed at 298 K. Data represent mean ± SD from at least three independent experiments. Agonistic activity was determined by measuring the PqsR stimulation induced by 100 μM of the test compound compared to 50 nM PQS (=100%); n.a. = no agonism (agonistic activity ≤10%). Antagonistic activity was determined by measuring the inhibition of the PqsR stimulation induced by 50 nM PQS in the presence of 100 μM test compound (full inhibition =100%); n.i. = no inhibition (antagonistic activity ≤10%). Mean value of at least two independent experiments with $n = 4$, standard deviation less than 25%. Significance: for the agonist test, induction compared to the basal value; for the antagonist test, decrease of the PQS-induced induction. [b]$p < 0.003$. [c]$p < 0.05$.

the resulting PqsR Q194A mutant was analyzed by ITC (Table 2).

Table 2. Effect of the Q194A Mutation on the Thermodynamic Parameters of Ligand Binding[a]

ligand	$\Delta\Delta G$ [kcal mol^{-1}]	$\Delta\Delta H$ [kcal mol^{-1}]	$-T\Delta\Delta S$ [kcal mol^{-1}]
1	0.0 ± 0.1	0.1 ± 0.1	−0.1 ± 0.1
8	−1.3 ± 0.3[b]	−4.0 ± 0.3[b]	2.7 ± 0.4[b]
9	−1.3 ± 0[b]	−4.4 ± 0.3[b]	3.1 ± 0.3[b]
11	−0.5 ± 0.1[b]	−4.1 ± 0.4[b]	3.6 ± 0.4[b]

[a]$\Delta\Delta G$, $\Delta\Delta H$, and $-T\Delta\Delta S$ are $\Delta G_{WT} - \Delta G_{mutant}$, $\Delta H_{WT} - \Delta H_{mutant}$, and $-T(\Delta S_{WT} - \Delta S_{mutant})$, respectively. Negative values indicate a loss; positive values, a gain compared to wild-type. Errors indicate SD calculated *via* Gaussian error propagation. Significance: effect of the Q194A mutation on the thermodynamic parameters of ligand binding compared to the wild-type. [b]$p < 0.003$.

While the Q194A mutation did not affect the binding of **1**, the affinity of **8**, **9**, and **11** was significantly decreased. The latter reveals that Gln194 is only involved in the binding of **8**, **9**, and **11**, but competition experiments confirmed that **1** and **11** bind to the same binding site (Supplementary Figure S5). Interestingly, for the interaction of **8**, **9**, and **11** with the Q194A mutant, a comparable loss in ΔH was observed with values ranging from 4.0 to 4.4 kcal mol^{-1}. Considering that a well-placed H-bond can make a favorable enthalpic contribution in the order of −4 to −5 kcal mol^{-1},[25] the results suggest that Gln194 forms H-bonds with **8**, **9**, and **11**. Further, the binding of the latter ligands to the Q194A mutant showed positive $-T\Delta\Delta S$ values relative to those of the wild-type. This might be due to the increased conformational flexibility both of the ligand and the protein in the absence of the H-bond.

As shown in Table 1, variation of the alkyl chain (compounds **6**−**10**) affects the enthalpy ΔH, demonstrating that the alkyl chain is involved in the formation of noncovalent interactions like CH/π hydrogen bonds. The latter have their origin in dispersion forces, which have an impact on the enthalpic term of free energy.[26] To probe for CH/π interactions Phe221 that is lining the PQS-binding pocket (Williams, P. University of Notthingham, Nottingham, U.K. Personal communication, 2011) was mutated to Ala. Ligand **9**, which showed the highest affinity toward PqsR (K_D = 0.9 μM), was selected for analysis, and the thermodynamic signatures for the binding of **9** to wild-type and F221A mutant PqsR are shown in Figure 3.

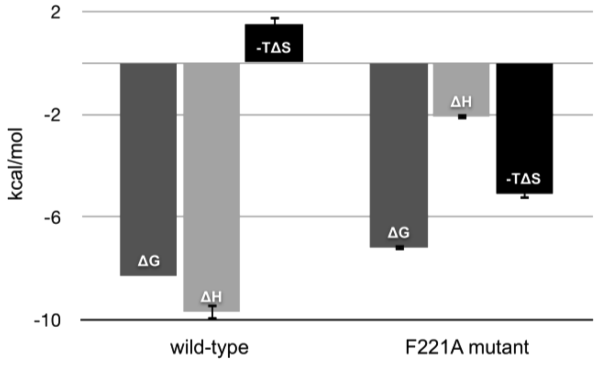

Figure 3. Thermodynamic profiles determined by ITC for the binding of ligand **9** to wild-type and F221A mutant PqsR. Data shown are mean ± SD, $n = 3$.

Indeed, the F221A point mutation affected the binding of **9**, and with a deficit of 7.6 kcal mol^{-1} the enthalpic contribution was significantly reduced compared to that of the wild-type. A salient feature of the CH/π hydrogen bond is that it works cooperatively and for cases involving aliphatic CH groups as the hydrogen donor, the energy of a CH/π hydrogen bond is between −1.5 and −2.5 kcal mol^{-1}.[27] This indicates that Phe221 might form three CH/π bonds with the *t*Bu moiety of **9** as described for the interaction of benzene with isobutane.[28]

Given that *P. aeruginosa* is characterized by an intrinsic resistance to a variety of antimicrobial agents, which is due to the synergy between drug efflux pumps with broad substrate specificity and low outer membrane permeability,[29] we examined whether the most potent antagonist **11** also shows

an effect when tested in a *P. aeruginosa* background. Remarkably, the antagonistic activity could be confirmed (IC_{50} in *E. coli* = 12.5 μM *vs* IC_{50} in *P. aeruginosa* = 23.6 μM; Supplementary Figure S6). Two possible explanations for this finding might be that the penetration of the hydrophilic hydroxamic acid **11** (log *P* = 2.1; calculated with MOE2010.10) across the outer membrane overwhelms its efflux or that the antagonist **11** is no substrate of the efflux pumps. Additionally, **11** is able to reduce the production of the virulence factor pyocyanin in *P. aeruginosa* (IC_{50} = 87.2 μM; Supplementary Figure S7).

In summary, through application of rational design and biophysical methods, we developed to the best of our knowledge the first small-molecule PqsR ligands. LEs and functional properties were used to guide the elaboration process that resulted in the potent hydroxamic acid-derived PqsR antagonist **11**. Compared to the recently described HHQ analogues[14] compound **11** is a less potent antagonist but, as a consequence of its low molecular weight and its activity in *P. aeruginosa*, it has high potential for further optimization. Beyond this, site-directed mutagenesis together with thermodynamic analysis disclosed that Gln194 and Phe221 are involved in ligand binding, probably by making hydrogen bonds and CH/π interactions, respectively. The rational simplification strategy in combination with biophysical methods, using LE as a primary filter, revealed promising hits. Accordingly, this approach is a valuable tool in drug design. Future experiments will address hit to lead optimization to open the door for anti-infectives with novel modes of action for the treatment of *P. aeruginosa* infections.

METHODS

Construction of pSUMO3_ck4_*pqsR*^{C87}. For generation of pSUMO3_ck4_*pqsR*^{C87} containing the truncated *pqsR*^{C87} gene of *P. aeruginosa* PA14, the *pqsR* gene from nucleotide 259 to the stop codon was PCR-amplified from genomic DNA using the forward primer 5′-TATGAGTACTAATCTCAACAAGGGTCCGCGC-3′ and reverse primer 5′-TGTACAATTGCTACTCTGGTGCGGCGCGCT-3′ (*Sca*I/*Mfe*I sites underlined) and subsequently cloned into the *Sca*I/*Mfe*I sites of the pSUMO3_ck4 vector in order to express it as a H_6SUMO-fusion protein. The construct was confirmed by DNA sequencing. This plasmid adds 104 amino acids to the N-terminus of the PqsR sequence starting at N87 .

Preparation of pSUMO3_ck4_Q194A*pqsR*^{C87} and pSUMO3_ck4_F221A*pqsR*^{C87}. The Q194A and the F221A mutants were generated using the QuikChange Site-Directed Mutagenesis Kit (Stratagene) according to the manufacturer's instructions using the pSUMO3-ck4-*pqsR*^{C87} plasmid as an template. Briefly, the forward primer 5′-CTGGCCAATTACCGGGCGATCAGCCTCGGCAGC-3′ (A194 underlined) and the reverse primer 5′-GCTGCCGAGGCTGATCGCCCGGTAATTGGCCAG-3′ (A194 underlined) were used to amplify the Q194A gene through 16 cycles of PCR (35 s denaturation at 95 °C, 60 s annealing at 55 °C, and 6.5 min extension at 68 °C). The forward primer 5′-CTCTTCGTGGAAAACGCGGACGACATGCTGCGTCTG-3′ (A221 underlined) and the reverse primer 5′-CAGACGCAGCATGTCGTCCGCGTTTTCCACGAAGAG-3′ (A221 underlined) were used to amplify the F221A gene through 16 cycles of PCR using the same conditions as described above. After treatment with *Dpn*I, the PCR product was transformed into *E. coli* strain XL1-Blue. Plasmid DNA was then purified from transformants using the GenElute HP Plasmid Miniprep Kit (Sigma-Aldrich) and sequenced to confirm the Q194A and the F221A mutations.

Protein Expression and Purification. Wild-type, Q194A mutant, and F221A mutant H_6SUMO-PqsR^{C87} were expressed in *E. coli* and purified using a single affinity chromatography step. Briefly, *E. coli* BL21 (DE3) cells containing the pSUMO3_ck4_*pqsR*^{C87}, the pSUMO3_ck4_Q194A*pqsR*^{C87}, or the pSUMO3_ck4_F221A*pqsR*^{C87} plasmid were grown in LB medium containing 50 μg mL^{-1} kanamycin at 37 °C to an OD_{600} of approximately 0.8 and induced with 0.2 mM IPTG for 16 h at 16 °C. The cells were harvested by centrifugation (5000 rpm, 10 min, 4 °C), and the cell pellet was resuspended in 100 mL of binding buffer (50 mM Tris-HCl, pH 7.8, 150 mM NaCl, 20 mM imidazole, 10% glycerol (v/v)) and lysed by sonication for a total process time of 2.5 min. Cell debris were removed by centrifugation (13000 rpm, 30 min), and the supernatant was filtered through a syringe filter (0.2 μm). The clarified lysate was immediately applied to a Ni-NTA column (GE Healthcare), washed with 50 mM Tris-HCl, pH 7.8, 150 mM NaCl, 20 mM imidazole, 10% glycerol (v/v), and eluted with 500 mM imidazole. The protein-containing fractions were buffer-exchanged into 20 mM Tris, pH 7.4, 150 mM NaCl, 10% glycerol (v/v) for the wild-type and into 20 mM Tris, pH 7.8, 300 mM NaCl, 10% glycerol (v/v) for the Q194A and the F221A mutants, using a PD10 column (GE Healthcare), and judged pure by SDS-PAGE analysis. The H_6SUMO-tagged proteins were stored at −80 °C and used for biophysical studies.

Minimal Biotinylation of H_6SUMO-PqsR^{C87}. Minimal biotinylation of the H_6SUMO-PqsR^{C87} was achieved by mixing 56 nmol of H_6SUMO-PqsR^{C87} (1 equiv) with 28 nmol of EZ-link sulfoNHS LC-LC-biotin (0.5 equiv.; Thermofisher Scientific) that was freshly dissolved in water. Biotinylation reaction mixture was incubated on ice for 2 h. To remove unreacted biotin reagent, the entire biotinylation mixture was subjected to size exclusion chromatography on a Superdex 200HR (16/600) column equilibrated in storage buffer (1× PBS, pH 7.4, 10% glycerol (v/v)). A protein peak containing biotinylated H_6SUMO-PqsR^{C87} protein was collected (0.3 mg mL^{-1}), stored at −80 °C, and used for SPR studies.

Surface Plasmon Resonance. SPR binding studies were performed using a Reichert SR7500DC instrument optical biosensor (Reichert Technologie). SAD500 sensor chips from Xantec Analytics were used. Dimethyl sulfoxide (DMSO), biotin, and (±)-*trans*-U50488 methanesulfonate were purchased from Sigma. The library collection consisted of 106 compounds with molecular weight range of 100−350 Da.

Immobilization of Biotinylated H_6Sumo-PqsR^{C87}. Biotinylated H_6SUMO-PqsR^{C87} was immobilized on a SAD500 (Streptavidin coated) sensor chip at 25 °C. HEPES (50 mM HEPES, pH 7.4, 150 mM NaCl) was used as the running buffer. The streptavidin carboxymethyl dextran surface was preconditioned 30 min with running buffer until the baseline was stable. Biotinylated H_6SUMO-PqsR^{C87} was diluted into running buffer to a concentration of 100 μg mL^{-1} and coupled to the surface with a 2-min injection. Remaining streptavidin and the reference cell were blocked with a 3-min injection of biotin (3 μg mL^{-1}). Biotinylated H_6SUMO-PqsR^{C87} (39494 Da) was immobilized at a density of 2200 RU for the binding affinity experiment of (±)-*trans*-U50488 methanesulfonate, at a density of 5506 RU for the library screen and at a density of 3092 RU for competition experiments.

Binding Affinity for (±)-*trans*-U50488 Methanesulfonate. The binding experiment was performed at 12 °C at a constant flow rate of 80 μL min^{-1} in instrument running buffer (50 mM HEPES, 150 mM NaCl, pH 7.4, 5% DMSO (v/v), 0.05% P20 (v/v). A 10 mM stock of *trans*-U50488 methanesulfonate in running buffer was directly diluted to a concentration of 1 mM and then diluted in a 3-fold dilution series from 111 μM down to 457 nM. Before starting the experiments 12 warm-up blank injections were performed. Zero-buffer blank injections and DMSO calibrations were included for double referencing. Individual concentrations were injected in duplicates from lowest to highest concentrations for 120 s association and 5 min dissociation time. Scrubber software was used for processing and analyzing data. Equilibrium dissociation constant (K_D) was determined by locally fitting appropriate experimental data to a 1:1 model using the fitting procedure available within Scrubber software. Overlay plot of sensorgrams and affinity plot in adequate logarithmic units for the concentrations[30] are shown in Supplementary Figure S1.

Library Screening. Concentrations of ligand stock solutions in DMSO were determined by the weight of the compound. Compounds as 10 mM DMSO stocks were diluted in DMSO to 2 mM. Final ligand concentrations (100 μM) were achieved by diluting 1:20 (v/v) in the experimental buffer (50 mM HEPES, pH 7.4, 150 mM NaCl, 0.05% P20 (v/v)) resulting in a final DMSO concentration of 5% (v/v). Binding experiments were performed at 12 °C at a constant flow rate of 100 μL min^{-1} in instrument running buffer (50 mM HEPES, pH 7.4, 150 mM NaCl, 5% DMSO (v/v), 0.05% P20 (v/v). Each compound was injected for 26 s association time and 120 s dissociation time. Positive control ((±)-*trans*-U50488 methanesulfonate) was injected each 25th injection at 20 μM to assess stability and reproducibility of the assay, and 110 compounds were screened within 6 h in 96-well plates. Data evaluation was performed using Scrubber (http://www.biologic.com.au) and Microsoft Excel software for data processing and analysis. Using Scrubber software, SPR signals in the flow cell containing captured biotinylated protein were transformed, referenced against the blank surface (streptavidin), and further corrected for DMSO refractive index change (excluded volume effect). Compounds showing promiscuous binding response[31] were removed from the screening data. Report binding points, taken for each fragment injection after a contact interval of 19-s were analyzed. K_D values were estimated using eq 1 derived from the Langmuir adsorption isotherm:

$$K_D = (R_{max}C/R) - C \quad (1)$$

R_{max}, R, and C correspond to the normalized saturation response of the compound, the normalized response of the test compound, and the concentration of the test solution, respectively. For the ranking of the best hits, the LE was calculated as previously described[18,32] from eq 2:

$$LE = -RT \ln K_D/(\text{heavy atom count}) \quad (2)$$

T is the absolute temperature, and R = 1.98 cal mol^{-1} K^{-1}.

Overlay of sensorgrams for compounds binding to H_6SUMO-PqsR^{C87} surface and data read out line is shown in Supplementary Figure S8.

Competition Experiments for (±)-*trans*-U50488 Methanesulfonate and Compound 11. The competition experiment was performed at 12 °C at a constant flow rate of 25 μL min^{-1} in instrument running buffer (50 mM HEPES, 150 mM NaCl, pH 7.4, 5% DMSO (v/v), 0.05% P20 (v/v), 100 μM compound **11**. A 10 mM stock of *trans*-U50488 methanesulfonate in running buffer was directly diluted to a concentration of 1 mM and then diluted in a 3-fold dilution series from 333 μM down to 4.57 μM. Before starting the experiments 12 warm-up blank injections were performed. Zero-buffer blank injections and DMSO calibrations were included for double referencing. Individual concentrations were injected in duplicates from lowest to highest concentrations for 120 s association time and 5 min dissociation time. Scrubber software was used for processing and analyzing data. Equilibrium dissociation constant (K_D) was determined by locally fitting appropriate experimental data to a 1:1 model using the fitting procedure available within Scrubber software. Overlay plot of sensorgrams and affinity plot in adequate logarithmic units for the concentrations[30] are shown in Supplementary Figure S6.

Isothermal Titration Calorimetry. ITC experiments were carried out using an ITC_{200} instrument (Microcal Inc., GE Healthcare). Concentrations of ligand stock solutions in DMSO were determined by the weight of the compound. Final ligand concentrations were achieved by diluting 1:20 (v/v) in the experimental buffer resulting in a final DMSO concentration of 5% (v/v). Protein concentration was determined by measuring the absorbance at 280 nm using a theoretical molarity extinction coefficient of 22,900 M^{-1} cm^{-1}. DMSO concentration in the protein solution was adjusted to 5% (v/v). ITC measurements were routinely performed at 25 °C in 20 mM Tris, pH 7.4, 150 mM NaCl, 10% glycerol (v/v), 5% DMSO (v/v) for the wild-type PqsR^{C87}and in 20 mM Tris, pH 7.4, 300 mM NaCl, 10% glycerol (v/v), 5% DMSO (v/v) for the Q194A and the F221A mutants, respectively. The titrations were performed on 66−200 μM H_6SUMO-PqsR^{C87}, H_6SUMO-Q194APqsR^{C87}, or H_6SUMO-F221APqsR^{C87} in the 200 μL sample cell using 2−2.7 μL injections of 0.7−2.5 mM ligand solution every 180 s. The competition experiment was performed on 94 μM H_6SUMO-PqsR^{C87}, which was incubated with 1 mM compound **1** for 30 min at 25 °C. Raw data were collected and, the area under each peak was integrated. To correct for heats of dilution and mixing the final baseline consisting of small peaks of the same size at the end of the experiment was subtracted. The experimental data were fitted to a theoretical titration curve (one site binding model) using MicroCal Origin 7 software, with ΔH (enthalpy change in kcal mol^{-1}), K_A (association constant in M^{-1}), and N (number of binding sites) as adjustable parameters. Thermodynamic parameters were calculated from eq 3:

$$\Delta G = \Delta H - T\Delta S = RT \ln K_A = -RT \ln K_D \quad (3)$$

where ΔG, ΔH, and ΔS are the changes in free energy, enthalpy, and entropy of binding, respectively, T is the absolute temperature, and R = 1.98 cal mol^{-1} K^{-1}. The LE for each compound was calculated from eq 4:

$$LE = -\Delta G/(\text{heavy atom count}) \quad (4)$$

where ΔG is the change in free energy and heavy atom count is the number of non-hydrogen atoms of the compound. For each ligand at least three independent experiments were performed. Representative ITC titrations of **1**, **8**, and **11** against H_6SUMO-PqsR^{C87} and H_6SUMO-Q194APqsR^{C87} are shown in Supplementary Figure S2. Representative ITC titrations of **9** against H_6SUMO-PqsR^{C87}, H_6SUMO-Q194APqsR^{C87}, and H_6SUMO-F221APqsR^{C87} are shown in Supplementary Figure S9. Representative ITC titrations of **4**, **6**, **7**, **10**, and **12** against H_6SUMO-PqsR^{C87} are shown in Supplementary Figure S10.

Synthesis. Complete chemical and analytical methods are described in the Supporting Information.

Reporter Gene Assays. The β-galactosidase reporter gene assays in *E.coli* and *P. aeruginosa* PA14 were performed as previously described and are explained into details in the Supporting Information.

Pyocyanin Assay. The pyocyanin assay in *P. aeruginosa* PA14 was performed as previously described and is explained into details in the Supporting Information.

■ ASSOCIATED CONTENT

Ⓢ Supporting Information

Synthetic and analytical methods for the compounds described herein; detailed description of the reporter gene assays and pyocyanin assay; Supplementary Figures S1−S10. This material is available free of charge *via* the Internet at http://pubs.acs.org.

■ AUTHOR INFORMATION

Corresponding Author

*E-mail: rolf.hartmann@helmholtz-hzi.de.

Author Contributions

#These authors contributed equally to this work.

Notes

The authors declare no competing financial interest.

■ ACKNOWLEDGMENTS

The authors thank S. Amann for her help in performing the reporter gene assay. We are very grateful to C. Cugini and D. Hogan (Dartmouth Medical School, Hanover, NH, USA) for kindly supplying the plasmid pEAL08-2. The *P. aeruginosa* PA14 strain was kindly provided by S. Häussler (Helmholtz Centre for Infection Research, Braunschweig, Germany).

■ REFERENCES

(1) Blanc, D. S., Petignat, C., Janin, B., Bille, J., and Francioli, P. (1998) Frequency and molecular diversity of Pseudomonas aeruginosa upon admission and during hospitalization: a prospective epidemiologic study. *Clin. Microbiol. Infect.* 4, 242−247.

(2) Koch, C., and Høiby, N. (1993) Pathogenesis of cystic fibrosis. *Lancet 341*, 1065−1069.
(3) Swift, S., Downie, J. A., Whitehead, N. A., Barnard, A. M., Salmond, G. P., and Williams, P. (2001) Quorum sensing as a population-density-dependent determinant of bacterial physiology. *Adv. Microb. Physiol. 45*, 199−270.
(4) Gambello, M. J., and Iglewski, B. H. (1991) Cloning and characterization of the Pseudomonas aeruginosa lasR gene, a transcriptional activator of elastase expression. *J. Bacteriol. 173*, 3000−3009.
(5) Passador, L., Cook, J. M., Gambello, M. J., Rust, L., and Iglewski, B. H. (1993) Expression of Pseudomonas aeruginosa virulence genes requires cell-to-cell communication. *Science 260*, 1127−1130.
(6) Ochsner, U. A., Koch, A. K., Fiechter, A., and Reiser, J. (1994) Isolation and characterization of a regulatory gene affecting rhamnolipid biosurfactant synthesis in Pseudomonas aeruginosa. *J. Bacteriol. 176*, 2044−2054.
(7) Ochsner, U. A., and Reiser, J. (1995) Autoinducer-mediated regulation of rhamnolipid biosurfactant synthesis in Pseudomonas aeruginosa. *Proc. Natl. Acad. Sci. U.S.A. 92*, 6424−6428.
(8) Pesci, E. C., Milbank, J. B., Pearson, J. P., McKnight, S., Kende, A. S., Greenberg, E. P., and Iglewski, B. H. (1999) Quinolone signaling in the cell-to-cell communication system of Pseudomonas aeruginosa. *Proc. Natl. Acad. Sci. U.S.A. 96*, 11229−11234.
(9) Allesen-Holm, M., Barken, K. B., Yang, L., Klausen, M., Webb, J. S., Kjelleberg, S., Molin, S., Givskov, M., and Tolker-Nielsen, T. (2006) A characterization of DNA release in Pseudomonas aeruginosa cultures and biofilms. *Mol. Microbiol. 59*, 1114−1128.
(10) Dubern, J.-F., and Diggle, S. P. (2008) Quorum sensing by 2-alkyl-4-quinolones in Pseudomonas aeruginosa and other bacterial species. *Mol. Biosyst. 4*, 882−888.
(11) Déziel, E., Gopalan, S., Tampakaki, A. P., Lépine, F., Padfield, K. E., Saucier, M., Xiao, G., and Rahme, L. G. (2005) The contribution of MvfR to Pseudomonas aeruginosa pathogenesis and quorum sensing circuitry regulation: multiple quorum sensing-regulated genes are modulated without affecting lasRI, rhlRI or the production of *N*-acyl-L-homoserine lactones. *Mol. Microbiol. 55*, 998−1014.
(12) Clatworthy, A. E., Pierson, E., and Hung, D. T. (2007) Targeting virulence: a new paradigm for antimicrobial therapy. *Nat. Chem. Biol. 3*, 541−548.
(13) Xiao, G., Déziel, E., He, J., Lépine, F., Lesic, B., Castonguay, M.-H., Milot, S., Tampakaki, A. P., Stachel, S. E., and Rahme, L. G. (2006) MvfR, a key Pseudomonas aeruginosa pathogenicity LTTR-class regulatory protein, has dual ligands. *Mol. Microbiol. 62*, 1689−1699.
(14) Lu, C., Kirsch, B., Zimmer, C., de Jong, J. C., Henn, C., Maurer, C. K., Müsken, M., Häussler, S., Steinbach, A., and Hartmann, R. W. (2012) Discovery of antagonists of PqsR, a key player in 2-alkyl-4-quinolone-dependent quorum sensing in Pseudomonas aeruginosa. *Chem. Biol. 19*, 381−390.
(15) Zaborina, O., Lepine, F., Xiao, G., Valuckaite, V., and Chen, Y. (2007) Dynorphin activates quorum sensing quinolone signaling in Pseudomonas aeruginosa. *PLoS Pathog. 3*, e35.
(16) Mochalkin, I., Miller, J. R., Narasimhan, L., Thanabal, V., Erdman, P., Cox, P. B., Prasad, J. V. N. V., Lightle, S., Huband, M. D., and Stover, C. K. (2009) Discovery of antibacterial biotin carboxylase inhibitors by virtual screening and fragment-based approaches. *ACS Chem. Biol. 4*, 473−483.
(17) Waldrop, G. L. (2009) Smaller is better for antibiotic discovery. *ACS Chem. Biol. 4*, 397−399.
(18) Hopkins, A. L., Groom, C. R., and Alex, A. (2004) Ligand efficiency: a useful metric for lead selection. *Drug Discovery Today 9*, 430−431.
(19) Abad-Zapatero, C., and Metz, J. T. (2005) Ligand efficiency indices as guideposts for drug discovery. *Drug Discovery Today 10*, 464−469.
(20) Cugini, C., Calfee, M. W., Farrow, J. M., Morales, D. K., Pesci, E. C., and Hogan, D. A. (2007) Farnesol, a common sesquiterpene, inhibits PQS production in Pseudomonas aeruginosa. *Mol. Microbiol. 65*, 896−906.
(21) Fletcher, M. P., Diggle, S. P., Crusz, S. A., Chhabra, S. R., Cámara, M., and Williams, P. (2007) A dual biosensor for 2-alkyl-4-quinolone quorum-sensing signal molecules. *Environ. Microbiol. 9*, 2683−2693.
(22) Hodgkinson, J., Bowden, S. D., Galloway, W. R. J. D., Spring, D. R., and Welch, M. (2010) Structure-activity analysis of the Pseudomonas quinolone signal molecule. *J. Bacteriol. 192*, 3833−3837.
(23) Ladbury, J. E., Klebe, G., and Freire, E. (2010) Adding calorimetric data to decision making in lead discovery: a hot tip. *Nat. Rev. Drug Discovery 9*, 23−27.
(24) Ciulli, A., Williams, G., Smith, A. G., Blundell, T. L., and Abell, C. (2006) Probing hot spots at protein−ligand binding sites: A fragment-based approach using biophysical methods. *J. Med. Chem. 49*, 4992−5000.
(25) Freire, E. (2008) Do enthalpy and entropy distinguish first in class from best in class? *Drug Discovery Today 13*, 869−874.
(26) Ramírez-Gualito, K., Alonso-Ríos, R., Quiroz-García, B., Rojas-Aguilar, A., Díaz, D., Jiménez-Barbero, J., and Cuevas, G. (2009) Enthalpic nature of the CH/pi interaction involved in the recognition of carbohydrates by aromatic compounds, confirmed by a novel interplay of NMR, calorimetry, and theoretical calculations. *J. Am. Chem. Soc. 131*, 18129−18138.
(27) Nishio, M. (2011) The CH/π hydrogen bond in chemistry. Conformation, supramolecules, optical resolution and interactions involving carbohydrates. *Phys. Chem. Chem. Phys. 13*, 13873−13900.
(28) Ran, J., and Wong, M. W. (2006) Saturated hydrocarbon-benzene complexes: theoretical study of cooperative CH/pi interactions. *J. Phys. Chem. A 110*, 9702−9709.
(29) Ma, D., Cook, D. N., Hearst, J. E., and Nikaido, H. (1994) Efflux pumps and drug resistance in gram-negative bacteria. *Trends Microbiol. 2*, 489−493.
(30) Rich, R. L., and Myszka, D. G. (2010) Grading the commercial optical biosensor literature-Class of 2008: The Mighty Binders. *J. Mol. Recognit. 23*, 1−64.
(31) Giannetti, A. M., Koch, B. D., and Browner, M. F. (2008) Surface plasmon resonance based assay for the detection and characterization of promiscuous inhibitors. *J. Med. Chem. 51*, 574−580.
(32) Navratilova, I., and Hopkins, A. L. (2010) Fragment screening by surface plasmon resonance. *ACS Med. Chem. Lett. 1*, 44−48.